

Observation of a threshold enhancement in the $p\bar{\Lambda}$ invariant mass spectrum

M. Ablikim¹, J. Z. Bai¹, Y. Ban¹⁰, J. G. Bian¹, X. Cai¹, J. F. Chang¹, H. F. Chen¹⁶, H. S. Chen¹, H. X. Chen¹, J. C. Chen¹, Jin Chen¹, Jun Chen⁶, M. L. Chen¹, Y. B. Chen¹, S. P. Chi², Y. P. Chu¹, X. Z. Cui¹, H. L. Dai¹, Y. S. Dai¹⁸, Z. Y. Deng¹, L. Y. Dong¹, S. X. Du¹, Z. Z. Du¹, J. Fang¹, S. S. Fang², C. D. Fu¹, H. Y. Fu¹, C. S. Gao¹, Y. N. Gao¹⁴, M. Y. Gong¹, W. X. Gong¹, S. D. Gu¹, Y. N. Guo¹, Y. Q. Guo¹, Z. J. Guo¹⁵, F. A. Harris¹⁵, K. L. He¹, M. He¹¹, X. He¹, Y. K. Heng¹, H. M. Hu¹, T. Hu¹, G. S. Huang^{1†}, L. Huang⁶, X. P. Huang¹, X. B. Ji¹, Q. Y. Jia¹⁰, C. H. Jiang¹, X. S. Jiang¹, D. P. Jin¹, S. Jin¹, Y. Jin¹, Y. F. Lai¹, F. Li¹, G. Li¹, H. H. Li¹, J. Li¹, J. C. Li¹, Q. J. Li¹, R. B. Li¹, R. Y. Li¹, S. M. Li¹, W. G. Li¹, X. L. Li⁷, X. Q. Li⁹, X. S. Li¹⁴, Y. F. Liang¹³, H. B. Liao⁵, C. X. Liu¹, F. Liu⁵, Fang Liu¹⁶, H. M. Liu¹, J. B. Liu¹, J. P. Liu¹⁷, R. G. Liu¹, Z. A. Liu¹, Z. X. Liu¹, F. Lu¹, G. R. Lu⁴, J. G. Lu¹, C. L. Luo⁸, X. L. Luo¹, F. C. Ma⁷, J. M. Ma¹, L. L. Ma¹¹, Q. M. Ma¹, X. Y. Ma¹, Z. P. Mao¹, X. H. Mo¹, J. Nie¹, Z. D. Nie¹, S. L. Olsen¹⁵, H. P. Peng¹⁶, N. D. Qi¹, C. D. Qian¹², H. Qin⁸, J. F. Qiu¹, Z. Y. Ren¹, G. Rong¹, L. Y. Shan¹, L. Shang¹, D. L. Shen¹, X. Y. Shen¹, H. Y. Sheng¹, F. Shi¹, X. Shi¹⁰, H. S. Sun¹, S. S. Sun¹⁶, Y. Z. Sun¹, Z. J. Sun¹, X. Tang¹, N. Tao¹⁶, Y. R. Tian¹⁴, G. L. Tong¹, G. S. Varner¹⁵, D. Y. Wang¹, J. X. Wang¹, J. Z. Wang¹, K. Wang¹⁶, L. Wang¹, L. S. Wang¹, M. Wang¹, P. Wang¹, P. L. Wang¹, S. Z. Wang¹, W. F. Wang¹, Y. F. Wang¹, Zhe Wang¹, Z. Wang¹, Zheng Wang¹, Z. Y. Wang¹, C. L. Wei¹, D. H. Wei³, N. Wu¹, Y. M. Wu¹, X. M. Xia¹, X. X. Xie¹, B. Xin⁷, G. F. Xu¹, H. Xu¹, Y. Xu¹, S. T. Xue¹, M. L. Yan¹⁶, F. Yang⁹, H. X. Yang¹, J. Yang¹⁶, S. D. Yang¹, Y. X. Yang³, M. Ye¹, M. H. Ye², Y. X. Ye¹⁶, L. H. Yi⁶, Z. Y. Yi¹, C. S. Yu¹, G. W. Yu¹, C. Z. Yuan¹, J. M. Yuan¹, Y. Yuan¹, Q. Yue¹, S. L. Zang¹, Yu. Zeng¹, Y. Zeng⁶, B. X. Zhang¹, B. Y. Zhang¹, C. C. Zhang¹, D. H. Zhang¹, H. Y. Zhang¹, J. Zhang¹, J. Y. Zhang¹, J. W. Zhang¹, L. S. Zhang¹, Q. J. Zhang¹, S. Q. Zhang¹, X. M. Zhang¹, X. Y. Zhang¹¹, Y. J. Zhang¹⁰, Y. Y. Zhang¹, Yiyun Zhang¹³, Z. P. Zhang¹⁶, Z. Q. Zhang⁴, D. X. Zhao¹, J. B. Zhao¹, J. W. Zhao¹, M. G. Zhao⁹, P. P. Zhao¹, W. R. Zhao¹, X. J. Zhao¹, Y. B. Zhao¹, Z. G. Zhao^{1*}, H. Q. Zheng¹⁰, J. P. Zheng¹, L. S. Zheng¹, Z. P. Zheng¹, X. C. Zhong¹, B. Q. Zhou¹, G. M. Zhou¹, L. Zhou¹, N. F. Zhou¹, K. J. Zhu¹, Q. M. Zhu¹, Y. C. Zhu¹, Y. S. Zhu¹, Yingchun Zhu¹, Z. A. Zhu¹, B. A. Zhuang¹, B. S. Zou¹.

(BES Collaboration)

¹ Institute of High Energy Physics, Beijing 100039, People's Republic of China

² China Center for Advanced Science and Technology (CCAST), Beijing 100080, People's Republic of China

³ Guangxi Normal University, Guilin 541004, People's Republic of China

⁴ Henan Normal University, Xinxiang 453002, People's Republic of China

⁵ Huazhong Normal University, Wuhan 430079, People's Republic of China

⁶ Hunan University, Changsha 410082, People's Republic of China

⁷ Liaoning University, Shenyang 110036, People's Republic of China

⁸ Nanjing Normal University, Nanjing 210097, People's Republic of China

⁹ Nankai University, Tianjin 300071, People's Republic of China

¹⁰ Peking University, Beijing 100871, People's Republic of China

¹¹ Shandong University, Jinan 250100, People's Republic of China

¹² Shanghai Jiaotong University, Shanghai 200030, People's Republic of China

¹³ Sichuan University, Chengdu 610064, People's Republic of China

¹⁴ Tsinghua University, Beijing 100084, People's Republic of China

¹⁵ University of Hawaii, Honolulu, Hawaii 96822

¹⁶ University of Science and Technology of China, Hefei 230026, People's Republic of China

¹⁷ Wuhan University, Wuhan 430072, People's Republic of China

¹⁸ Zhejiang University, Hangzhou 310028, People's Republic of China

* Visiting professor at the University of Michigan, Ann Arbor, MI 48109 USA

† Current address: Purdue University, West Lafayette, Indiana 47907, USA

(Dated: November 3, 2018)

An enhancement near the $m_p + M_\Lambda$ mass threshold is observed in the combined $p\bar{\Lambda}$ and $\bar{p}\Lambda$ invariant mass spectrum from $J/\psi \rightarrow pK^-\bar{\Lambda} + c.c.$ decays. It can be fit with an S-wave Breit-Wigner resonance with a mass $m = 2075 \pm 12$ (stat) ± 5 (syst) MeV and a width of $\Gamma = 90 \pm 35$ (stat) ± 9 (syst) MeV; it can also be fit with a P-wave Breit-Wigner resonance. Evidence for a similar enhancement is

also observed in $\psi' \rightarrow pK^-\bar{\Lambda} + c.c.$ decays. The analysis is based on samples of 5.8×10^7 J/ψ and 1.4×10^7 ψ' decays accumulated in the BES II detector at the Beijing Electron-Positron Collider.

PACS numbers: 12.39.Mk, 13.75.Ev, 12.40.Yx, 13.20.Gd

An anomalous enhancement near the mass threshold in the $p\bar{p}$ invariant mass spectrum was observed by the BES II experiment in $J/\psi \rightarrow \gamma p\bar{p}$ decays [1]. This enhancement can be fit with an S-wave Breit-Wigner resonance function with a mass around 1860 MeV and a width $\Gamma < 30$ MeV, and has been interpreted as a possible baryonium state [2]. Similar $p\bar{p}$ mass-threshold enhancements have been observed in the decays $B^+ \rightarrow K^+ p\bar{p}$ and $\bar{B}^0 \rightarrow D^0 p\bar{p}$ by the Belle Collaboration [3, 4]. These somewhat surprising experimental observations have stimulated a number of theoretical speculations [2, 5]. It is, therefore, of special interest to search for possible resonant structures in other baryon-antibaryon final states. The Belle Collaboration recently observed a near-threshold enhancement in the $p\bar{\Lambda}$ mass spectrum from $B \rightarrow p\bar{\Lambda}\pi$ decays [6]. In this letter, we report the observation of an enhancement near threshold in the $p\bar{\Lambda}$ invariant mass spectrum in $J/\psi \rightarrow pK^-\bar{\Lambda}$ and in $\psi' \rightarrow pK^-\bar{\Lambda}$ decays. (In this letter the inclusion of charge conjugate modes is always implied). The results are based on an analysis of 5.8×10^7 J/ψ and 1.4×10^7 ψ' decays detected in the upgraded Beijing Spectrometer (BESII) at the Beijing Electron-Positron Collider (BEPC).

BESII is a large solid-angle magnetic spectrometer that is described in detail in Ref.[7]. Charged particle momenta are determined with a resolution of $\sigma_p/p = 1.78\% \sqrt{1 + p^2(\text{GeV}^2)}$ in a 40-layer cylindrical main drift chamber (MDC). Particle identification is accomplished by specific ionization (dE/dx) measurements in the MDC and time-of-flight (TOF) measurements in a barrel-like array of 48 scintillation counters. The dE/dx resolution is $\sigma_{dE/dx} = 8.0\%$; the TOF resolution is measured to be $\sigma_{TOF} = 180$ ps for Bhabha events. Outside of the time-of-flight counters is a 12-radiation-length barrel shower counter (BSC) comprised of gas tubes interleaved with lead sheets. The BSC measures the energies and directions of photons with resolutions of $\sigma_E/E \simeq 21\%/\sqrt{E(\text{GeV})}$, $\sigma_\phi = 7.9$ mrad, and $\sigma_z = 2.3$ cm. The iron flux return of the magnet is instrumented with three double layers of counters that are used to identify muons. In this analysis, a GEANT3-based Monte Carlo (MC) package with detailed consideration of the detector performance (such as dead electronic channels) is used. The consistency between data and MC has been carefully checked in many high purity physics channels, and the agreement is reasonable.

The $J/\psi \rightarrow pK^-\bar{\Lambda}$ candidate events are required to have four charged tracks, each of which is well fitted to a helix within the polar angle region $|\cos\theta| < 0.8$ and with a transverse momentum larger than 50 MeV. The

total charge of the four tracks is required to be zero. For each track, the TOF and dE/dx information are combined to form particle identification confidence levels for the π , K and p hypotheses; the particle type of a track is assigned to be that of the hypothesis with the largest confidence level. In this analysis, reliable identification of the K^- is important. To have high efficiency, it is only required that one track be positively identified as a proton or antiproton. Events where the p , K^- , \bar{p} and π^+ tracks are all unambiguously identified are subjected to a four-constraint (4C) kinematic fit with the corresponding mass assignments for each track. For events with ambiguous particle identification, all possible 4C combinations are formed, and the combination with the smallest χ^2 is chosen. The final χ^2 is required to be less than 20. Further, the p and K^- tracks are required to originate near the interaction point, and the invariant mass of the $\bar{p}\pi^+$ combination is required to be less than 1.15 GeV. To suppress background events from $J/\psi \rightarrow pK^-\bar{\Sigma}^0$, we require $\xi = E_{miss} + 1.39M_{pK\text{ miss}} < 1.69$ GeV (see Fig. 1(a)), where E_{miss} denotes the difference between the center-of-mass energy (3.097 GeV) and the total energy of the four charged tracks, and $M_{pK\text{ miss}}$ denotes the mass recoiling against the proton-kaon system. This selection criterion is determined by optimizing the signal to background ratio based on Monte Carlo simulations. A sample of 5421 $J/\psi \rightarrow pK^-\bar{\Lambda}$ candidates survive the final selection. The $\bar{p}\pi^+$ invariant mass spectrum for these events, where a clear $\bar{\Lambda} \rightarrow \bar{p}\pi^+$ signal is evident, is shown in Fig. 1(b).

The $J/\psi \rightarrow pK^-\bar{\Lambda}$ events are experimentally quite distinct: they contain only charged tracks, three of which are heavy particles (i.e., p , \bar{p} and K), and the kinematics strongly constrains the event selection and mass assignments. In order to maintain a high selection efficiency and reduce systematic uncertainties, positive identification of only the proton or antiproton is required, and no requirement is placed on the Λ 's secondary vertex. The clean $\bar{\Lambda}$ signal in the $\bar{p}\pi^+$ invariant mass spectrum and good agreement with the $\bar{\Lambda}$ signal from a MC sample of $J/\psi \rightarrow pK^-\bar{\Lambda}$ events (Fig. 1(b)) indicate that the purity of the selected events is very high.

The level of background in the selected event sample was determined with two different MC studies. One used a specific set of background processes: $J/\psi \rightarrow pK^-\bar{\Sigma}^0$; $\Lambda\bar{\Lambda}$; $\Lambda\bar{\Lambda}\pi^0$; $p\bar{p}\pi^+\pi^-$; $p\bar{p}\pi^+\pi^-\pi^0$; and $\Sigma^0\bar{\Sigma}^0$, all produced according to branching ratios from Particle Data Group (PDG) Tables [8]. The fraction of these events that survive the $J/\psi \rightarrow pK^-\bar{\Lambda}$ selection criteria corresponds to about 18 events in the selected data sample. The second study used an inclusive MC sample of 30 million J/ψ events generated according to the LUND model [9]. This

study predicts that there are 56 background events in the data sample. These studies indicate that the background in the selected event sample is at the 1 ~ 2% level.

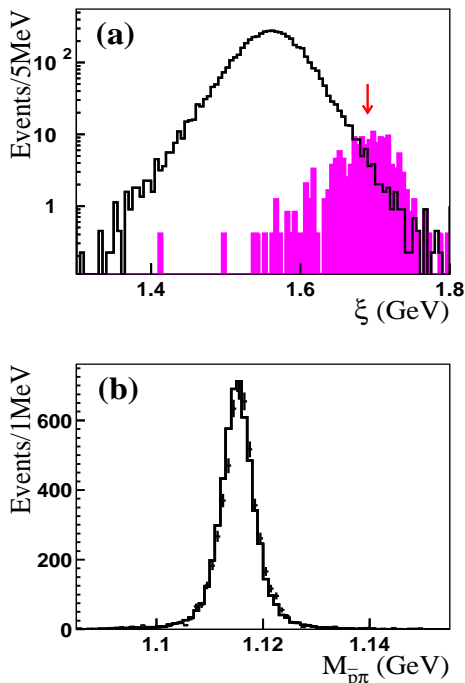


FIG. 1: (a) The ξ distribution (see text). The solid histogram denotes $J/\psi \rightarrow pK\bar{\Lambda}$ events, and the shaded histogram $J/\psi \rightarrow pK\bar{\Sigma}^0$ events, where both histograms are normalized to $5.8 \times 10^7 J/\psi$ events. Events with ξ values below the arrow are selected. (b) The $p\bar{\Lambda}$ invariant mass distribution for selected events; points with error bars denote the data and the histogram the MC (normalized to data).

The $p\bar{\Lambda}$ invariant mass spectrum for the selected events is shown in Fig. 2(a), where an enhancement is evident near the mass threshold. No corresponding structure is seen in a sample of $J/\psi \rightarrow pK\bar{\Lambda}$ MC events generated with a uniform phase space distribution. The $pK\bar{\Lambda}$ Dalitz plot is shown in Fig. 2(b). In addition to bands for the well established $\Lambda^*(1520)$ and $\Lambda^*(1690)$, there is a significant N^* band near the $K\bar{\Lambda}$ mass threshold, and a $p\bar{\Lambda}$ mass enhancement, isolated from the Λ^* and N^* bands, in the right-upper part of the Dalitz plot.

This enhancement can be fit with an acceptance weighted S-wave Breit-Wigner function [10], together with a function $f_{PS}(\delta)$ describing the phase space contribution, as shown in Fig. 2(c), where $f_{PS}(\delta) = N(\delta^{1/2} + a_1\delta^{3/2} + a_2\delta^{5/2})$, $\delta = m_{p\bar{\Lambda}} - m_p - m_{\bar{\Lambda}}$, and the parameters a_1 and a_2 are determined from a fit to the $pK\bar{\Lambda}$ MC sample events generated with a uniform phase-space distribution. The fit is confined to the $M_{p\bar{\Lambda}} - M_p - M_{\bar{\Lambda}} < 150$ MeV mass region and gives a peak mass of $m = 2075 \pm 12$ MeV and a width $\Gamma = 90 \pm 35$ MeV. The fit confidence level is 22.5% ($\chi^2/d.o.f. = 31.1/26$), and $-2\ln L = 29.9$. The no resonance hypothesis is also

tested, and the fit is much poorer: the confidence level is 5.5×10^{-10} ($\chi^2/d.o.f. = 101.5/29$), and $-2\ln L = 96.2$. This indicates that the enhancement deviates from the shape of the phase space contribution with a statistical significance of about 7σ .

The fit yields $N_{res} = 238 \pm 57$ signal events, corresponding to a branching ratio

$$\begin{aligned} & BR(J/\psi \rightarrow K^- X) BR(X \rightarrow p\bar{\Lambda}) \\ &= \frac{N_{res}/(2\epsilon BR(\Lambda \rightarrow p\pi))}{N_{J/\psi}} = (5.9 \pm 1.4) \times 10^{-5}, \end{aligned}$$

where $BR(\Lambda \rightarrow p\pi) = 63.9 \pm 0.5\%$ is taken from the PDG, $N_{J/\psi} = (5.77 \pm 0.27) \times 10^7$ is the total number of J/ψ events [11], and $\epsilon = 5.47 \pm 0.05\%$ is the MC-determined signal acceptance.

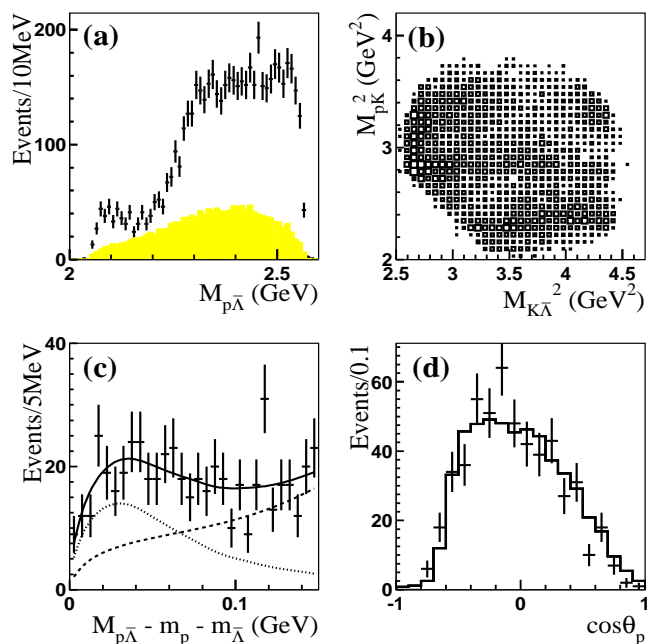


FIG. 2: (a) The points with error bars indicate the measured $p\bar{\Lambda}$ mass spectrum; the shaded histogram indicates phase space MC events (arbitrary normalization). (b) The Dalitz plot for the selected event sample. (c) A fit (solid line) to the data. The dotted curve indicates the Breit-Wigner signal and the dashed curve the phase space ‘background’. (d) The $\cos\theta_p$ distribution under the enhancement, the points are data and the histogram is the MC (normalized to data)

The signal acceptance and the phase space shape $f_{PS}(\delta)$ are corrected for differences between the low momentum p and \bar{p} tracking efficiencies for MC and data. The p and \bar{p} tracking efficiencies are measured with the data using a sample of $J/\psi \rightarrow p\bar{p}\pi^+\pi^-$ events.

A P-wave Breit-Wigner signal function (angular momentum $L = 1$) also gives an adequate fit to the data; here $\chi^2/d.o.f. = 32.5/26$ with a mass $M = 2044 \pm 17$ MeV and a width $\Gamma = 20 \pm 45$ MeV, which is consistent with zero. Fits with higher angular momentum

hypotheses $L \geq 2$ fail; such states are expected to be strongly suppressed near threshold.

The low acceptance for low momentum protons and anti-protons produces a non-uniform acceptance across the $M_{p\bar{\Lambda}} = 2075$ MeV band in the Dalitz plot (Fig. 2(b)). This is reflected in the non-uniform $\cos\theta_p$ distribution, where θ_p is the decay angle of p in the $p\bar{\Lambda}$ CM frame, for the events in the enhancement region ($M_{p\bar{\Lambda}} - M_p - M_{\bar{\Lambda}} < 150$ MeV), as shown in Fig. 2(d). The distribution agrees well with that of a MC sample of $J/\psi \rightarrow KX \rightarrow Kp\bar{\Lambda}$ with $M_X = 2075$ MeV and $\Gamma_X = 90$ MeV. Since the MC $\cos\theta_p$ distribution is generated as a uniform S-wave distribution, but the detected MC distribution agrees with data in Fig. 2(d), the observed distribution for the enhancement is consistent with S-wave decays to $p\bar{\Lambda}$.

Evidence of a similar enhancement is observed in $\psi' \rightarrow pK^-\bar{\Lambda}$, shown in Fig. 3 (a), when the same analysis is performed on the ψ' data sample. A fit is applied on the ψ' data sample with the $X(2075)$ parameters fixed at the values obtained from the J/ψ data, i.e., $M_X = 2075$ MeV and $\Gamma_X = 90$ MeV. The fit shows that the threshold enhancement in ψ' data deviates from the shape of the phase space contribution with a statistical significance of about 4.0σ , where the significance is estimated from a comparison of log-likelihood values of the fits with and without the $X(2075)$ signal function.

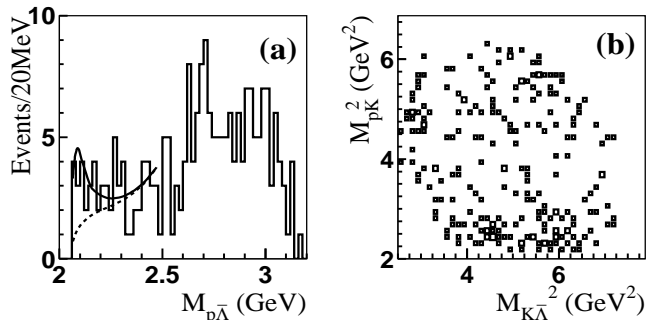


FIG. 3: Results for $\psi' \rightarrow pK^-\bar{\Lambda}$ events: (a) A fit (solid line) to the data sample (histogram); the dashed line indicates the phase space ‘background’ contribution. (b) The Dalitz plot.

The possibility that the enhancement in the J/ψ data sample is due to interference between N^* ’s and Λ^* ’s has been investigated with a partial wave analysis (PWA). The PWA results show that if the enhancement were from a pure interference effect, many large branching ratio J/ψ decays to N^* ’s and Λ^* ’s near the kinematic threshold are required, along with large mutual destructive interferences that cancel these large production rates [12]. Also, the similar enhancements seen in the ψ' data sample and in $B \rightarrow p\bar{\Lambda}\pi$ observed by the Belle experiment cannot be due to N^* and Λ^* interference effects since in these cases, contributions of the signal are far from the N^* and Λ^* bands in the Dalitz plot (See Fig. 3 (b)).

TABLE I: Systematic Errors

	mass(MeV)	width(MeV)	BR (%)
‘Background’ shape	4	8	27.3
Fitting bias	3	3	12.6
Particle identification			3.5
Tracking efficiency	0.3	1.2	12.6
χ^2			5.3
$N_{J/\psi}$			4.7
Total	5	9	33.5

Systematic uncertainties from different sources are studied. In the above fit, the phase space contribution is treated as the ‘background’ under the enhancement. Alternative ‘background’ shape parameters, including N^* ’s and Λ^* ’s contribution obtained from PWA fits, are used to estimate systematic uncertainties from the ‘background’ shape. The fitting bias near threshold is checked by MC studies. A set of MC samples combining a signal (resonance near threshold) process with a uniform phase space process are generated. In each MC sample, the mass, width and number of signal events are obtained from a fit using the same procedure as that done on the data. The averaged offsets between the fit output values and their input values are taken as one source of systematic uncertainty (fitting bias). The systematic uncertainty from the tracking efficiencies, especially from the low momentum p and \bar{p} tracks, are checked from data and MC comparisons, where the tracking efficiencies of p and \bar{p} are determined from a data sample of $J/\psi \rightarrow p\bar{p}\pi^+\pi^-$ events, and the tracking efficiencies of charged pions is obtained from $J/\psi \rightarrow \Lambda\bar{\Lambda}, \rho\pi$ events. The systematic uncertainty from the kinematic fit is estimated by using a different MDC wire resolution simulation model. Systematic uncertainties from other MC sources (such as mass resolution) are negligible. The systematic uncertainties determined from the above studies are listed in Table I, and the total systematic errors on the mass, width and branching ratios are 5 MeV, 9 MeV and 33.5% respectively.

In summary, an anomalous enhancement near threshold is observed in the invariant mass spectrum of $p\bar{\Lambda}$ in the $J/\psi \rightarrow pK^-\bar{\Lambda}$ and $\psi' \rightarrow pK^-\bar{\Lambda}$ processes. Both S-wave and P-wave Breit-Wigner resonance functions can fit the enhancement. If it is fitted with an S-wave Breit-Wigner resonance function, the mass is $m = 2075 \pm 12 \pm 5$ MeV, the width is $\Gamma = 90 \pm 35 \pm 9$ MeV, and the branching ratio is $BR(J/\psi \rightarrow K^-X)BR(X \rightarrow p\bar{\Lambda}) = (5.9 \pm 1.4 \pm 2.0) \times 10^{-5}$, where the first errors are statistical and the second are systematic. To understand the nature of this anomalous enhancement, searching for the same enhancement in $K\pi$ and $K\pi\pi$ modes in the $J/\psi, \psi' \rightarrow KK\pi, KK\pi\pi$ processes would help to distinguish whether it is from a conventional K^* meson or from a possible multi-quark state.

The BES collaboration acknowledges the staff of BEPC

for their hard efforts. This work is supported in part by the National Natural Science Foundation of China under contracts Nos. 19991480, 10225524, 10225525, the Chinese Academy of Sciences under contract No. KJ 95T-03, the 100 Talents Program of CAS under Contract Nos. U-11, U-24, U-25, and the Knowledge Innovation Project of CAS under Contract Nos. KJCX2-SW-N10, U-602, U-34 (IHEP); by the National Natural Science Foundation of China under Contract No. 10175060 (USTC); and by the Department of Energy under Contract No. DE-FG03-94ER40833 (U Hawaii).

-
- [1] BES Collaboration, J.Z. Bai *et al.*, Phys. Rev. Lett. **91**, 022001 (2003).
 [2] Alakabha Datta, Patrick J. O'Donnell, Phys. Lett. **B567**, 273(2003).
 [3] Belle Collaboration, K. Abe *et al.*, Phys. Rev. Lett. **88**, 181803 (2002).
 [4] Belle Collaboration, K. Abe *et al.*, Phys. Rev. Lett. **89**, 151802 (2002).
 [5] See, for example, J. Ellis, Y. Frishman and M. Karliner, Phys. Lett. **B566**, 201(2003); J.L. Rosner, Phys. Rev. D

- 68**, 014004 (2003); B.S. Zou and H.C. Chiang, Phys. Rev. D **69**, 034004 (2003).
 [6] Belle Collaboration, M.Z. Wang *et al.*, Phys. Rev. Lett. **90**, 201802 (2003).
 [7] BES Collaboration, J.Z. Bai *et al.*, Nucl. Instr. Meth. A **458**, 627 (2001).
 [8] Particle Data Group, K. Hagiwara *et al.*, Phys. Rev. D **66**, 010001 (2002).
 [9] J.C. Chen *et al.*, Phys. Rev. D **62**, 034003 (2000).
 [10] For the Breit-Wigner function, we use the form $BW(M) \propto \frac{q^{2L+1}k^3}{(M^2-M_0^2)^2+M_0^2\Gamma^2}$, where Γ is a constant (determined from the fit), q is the proton momentum in the $p\bar{\Lambda}$ frame, L is the $p\bar{\Lambda}$ orbital angular momentum, and k is the kaon momentum.
 [11] S.S. Fang *et al.*, HEP & Nucl. Phys. **27**, 277 (2003).
 [12] For example, from the PWA fit without X(2075), we can obtain the following estimation (using an acceptance about 10%): $BR(J/\psi \rightarrow p\bar{N}^*(2050))BR(\bar{N}^*(2050) \rightarrow K\bar{\Lambda}) \sim 0.3 \times 10^{-3}$, $BR(J/\psi \rightarrow \Lambda\bar{\Lambda}^*(1890)) \sim 0.8 - 1.5 \times 10^{-3}$, $BR(J/\psi \rightarrow \Lambda\bar{\Lambda}^*(1800)) \sim 1.5 - 2.5 \times 10^{-3}$, where $N^*(2050)(J^P = 3/2^+)$ is a new resonance and the other two are listed in the PDG. The above production of $\Lambda^*(1800)(J^P = 1/2^-)$ is via P-wave decays, and other two excited baryons can be produced via S-wave decays.